

Z. LIPNICKI*#, K. PANTOŁ**

ROLE OF THE CONTINUOUS CASTING FORMS ON THE SHAPE OF THE SOLIDIFIED CRUST

WPLYW GEOMETRII FORMY NA KSZTAŁT FRONTU KRZEPNIĘCIA PRZY ODLEWANIU CIĄGLYM

An analytical model for the transfer has been development and applied for calculating the shape of the solid thickness profile for continuous casting of a thin plate as an example. The stationary solidification front relative to the crystallizer was received from the superposition of the motions of the liquid metal flow in the axial direction and the solidifying metal in the perpendicular direction. The shape of the solidified crust was analyzed for different casting forms. The results are compared and graphically shown for different selected forms.

Keywords: continuous casting, solidification stationary front, shape of crust, contact layer

W pracy bada się analitycznie i oblicza kształty frontów krzepnięcia przy odlewaniu ciągłym cienkich płyt jako przykładu. Określono stacjonarne fronty krzepnięcia względem krystalizatora przez superpozycję dwóch ruchów: przepływu ciekłego metalu w kierunku pionowym i ruchu frontu krzepnięcia w kierunku poprzecznym. Wykazano zależność kształtu frontu krzepnięcia od parametrów termodynamicznych i przepływowych metalu. Rezultaty badań są porównane i przedstawione w formie graficznej dla wybranych kształtów odlewów.

Nomenclature

λ	thermal conductivity, $\text{Wm}^{-1}\text{K}^{-1}$
c	specific heat, $\text{Jkg}^{-1}\text{K}^{-1}$
ρ	density, kgm^{-3}
L	latent heat, Jkg^{-1}
u	mean velocity of the liquid metal flow, ms^{-1}
l	height of crystallizer, m
H	depth of crystallizer, m
T_F	liquid metal fusing point, K
T_0	temperature of cooling water, K
α_0	heat transfer coefficient between the channel wall and the cooling water, $\text{Wm}^{-2}\text{K}^{-1}$
α	heat transfer coefficient between liquid metal and crust, $\text{Wm}^{-2}\text{K}^{-1}$
α_{CON}	heat transfer coefficient between in contact layer, $\text{Wm}^{-2}\text{K}^{-1}$
T_W	surface temperature, K
t	time, s

x	vertical coordinate, m
δ	horizontal coordinate of the solidification front, m

1. Introduction

The continuous casting of alloy metals is a very valid and commonly known technology, which is described in detail in both the scientific and the professional literature for example in [1-7]. These papers present numerical methods for the calculation of a thick slab produced in a continuous casting process. For the continuous casting of thin plates specific conditions are present. The relatively low thermal resistance due to its small thickness compared to the thermal resistance contact layer allows it to use a simple analytical model to describe the phenomenon.

A special technology is applied for the continuous casting of thin metal rods. In [8] the slow solidification of a cylinder with a constant heat flux is analyzed. However, the development of the shape of the solidification front has not been investigated. In [9] the shape of the solidification crust has been investigated for thin metal rods. The shape and

* UNIVERSITY OF ZIELONA GÓRA, INSTITUTE OF ENVIRONMENTAL ENGINEERING, 65-516 ZIELONA GÓRA, POLAND

** STATE HIGHER VOCATION SCHOOL IN GŁOGÓW, 67-200 GŁOGÓW, POLAND

Corresponding author: z.lipnicki@iis.uz.zgora.pl

$$T_w = \frac{\alpha_{CON}}{\alpha_{CON} + \alpha_0} \bar{T} + \frac{\alpha_0}{\alpha_{CON} + \alpha_0} T_0 \quad \text{and} \quad (3)$$

$$\bar{T} = \frac{1}{1 + \frac{H - \delta}{\lambda} \cdot \frac{\alpha_0 \cdot \alpha_{CON}}{\alpha_0 + \alpha_{CON}}} T_F + \frac{1}{1 + \frac{\lambda}{H - \delta} \cdot \frac{\alpha_0 + \alpha_{CON}}{\alpha_0 \cdot \alpha_{CON}}} T_0 \quad (4)$$

After substituting the temperature T_w and \bar{T} given by equations (3) and (4) into equation (2) the following equation is obtained for the time depending thickness $H - \delta$, describing the position of the solidification front. Hereby the introducing the following dimensionless variables

$$Ste = \frac{c(T_F - T_0)}{L}; \quad \tau = SteFo; \quad Fo = \frac{at}{H^2}; \quad \tilde{\delta} = \frac{\delta}{H}; \quad (5)$$

$$\frac{1}{Bi_0} = \frac{\lambda}{\alpha_0 H}; \quad \frac{1}{Bi_{CON}} = \frac{\lambda}{\alpha_{CON} H}; \quad \mathcal{G} = \frac{\Delta T}{T_F - T_0} \frac{\alpha H}{\lambda}$$

which are respectively the Stephan number, a dimensionless time, the Fourier number, a dimensionless free channel width, the dimensionless thermal resistance for heat transfer to the coolant, the dimensionless thermal resistance of the contact layer and the parameter overheating have been introduced.

Equation (2) can be reduced as follows, after introducing the non-dimensional quantities

$$\mathcal{G} - \frac{d\tilde{\delta}}{d\tau} = \frac{1}{\beta + 1 - \tilde{\delta}}, \quad (6)$$

where the parameter β is equal to

$$\beta = \frac{1}{Bi_{CON}} + \frac{1}{Bi_0}.$$

This equation can be integrated after separation of variables to give the solidification time

$$\tau = \int_1^{\tilde{\delta}} \frac{\beta + 1 - \tilde{\delta}}{\mathcal{G}(\beta + 1 - \tilde{\delta}) - 1} d\tilde{\delta}, \quad (7)$$

and if the parameters β and \mathcal{G} are constants the above equation may be integrated

$$\tau = -\frac{1 - \tilde{\delta}}{\mathcal{G}} - \frac{1}{\mathcal{G}^2} \ln \frac{\mathcal{G}(\beta + 1 - \tilde{\delta}) - 1}{\beta \mathcal{G} - 1}. \quad (8)$$

The above simple equations fulfill the initial condition: $\tau = 0, \tilde{\delta} = 1$.

The solidification time depends on the position of the liquid metal flow relative to the inlet of the crystallizer (see Figure 2). At the inlet of the crystallizer ($x = 0$), the solidification time is equal to zero ($t = 0$) and increases with distance x according to equation (1). However, the solidification front is steady with respect to the crystallizer, because this situation results from the superposition of both motions: Liquid metal flow in the

axial direction x with the mean velocity u and the solidifying metal in the perpendicular direction. The solidification time is described by equation (1).

The above analysis shows that the steady state interface can be expressed by the following equations. From equations (1), (7) and (8) it follows

$$\tilde{x} = \frac{Re Pr a}{Ste} \int_1^{\tilde{\delta}} \frac{\beta + 1 - \tilde{\delta}}{\mathcal{G}(\beta + 1 - \tilde{\delta}) - 1} d\tilde{\delta} \quad \text{and} \quad (9)$$

$$\tilde{x} = -\frac{Re Pr \tilde{a}}{Ste} \left[\frac{1 - \tilde{\delta}}{\mathcal{G}} + \frac{1}{\mathcal{G}^2} \ln \frac{\mathcal{G}(\beta + 1 - \tilde{\delta}) - 1}{\beta \mathcal{G} - 1} \right].$$

In these equations, the dimensionless quantities are defined by

$$\tilde{x} = \frac{x}{H}, \quad Re = \frac{uH}{\nu}, \quad Pr = \frac{\nu}{a_l}, \quad \tilde{a} = \frac{a_l}{a}. \quad (10)$$

If liquid metal is not overheated $\mathcal{G} = 0$ the equation (6) takes the form

$$-\frac{d\tilde{\delta}}{d\tau} = \frac{1}{\beta + 1 - \tilde{\delta}}. \quad (11)$$

The solution of the above equation with the initial condition $\tau = 0, \tilde{\delta} = 1$ can be obtained to be

$$\tau = (\beta + 1)(1 - \tilde{\delta}) - \frac{1}{2}(1 - \tilde{\delta}^2) \quad \text{and}$$

$$\tilde{x} = \frac{Re Pr \tilde{a}}{Ste} \left[(\beta + 1)(1 - \tilde{\delta}) - \frac{1}{2}(1 - \tilde{\delta}^2) \right] \quad (12)$$

4. Results and discussion

The shapes of the solidified crusts for different casting forms (plate and rods), external conditions and different parameters of the liquid metal are given in Figures 3 and 4. Shapes of the solidification fronts for flat thin plates and thin rods are very different. This difference explains the rapidly decreasing heat flux for bars as compared to flat plates as you get closer to the axis of symmetry. In order to show the quantitative impact of the thermodynamic parameters on the solidification process the corresponding graphs are prepared.

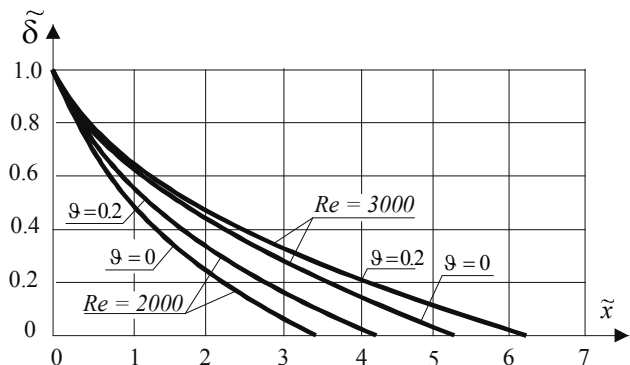


Fig. 3. Solidification front for a liquid metal for thin plat, $Pr = 0.01, Ste = 4, \beta = 0.2, \tilde{a} = 1.0$

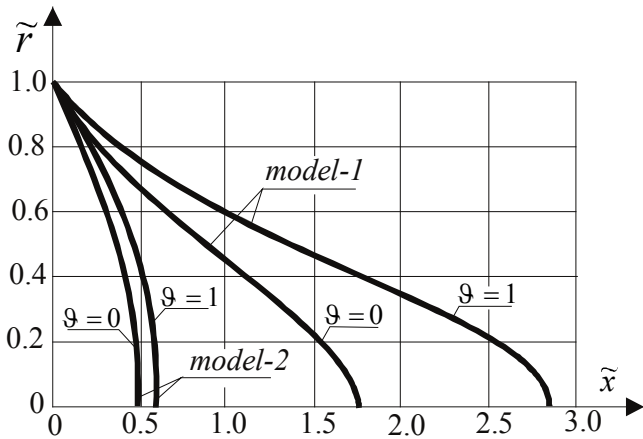


Fig. 4. Solidification front for a liquid metal for thin rods, $Pr=0.01, \beta=0.2, Re=2000, Ste=4, \tilde{a}=1.0$ [9]

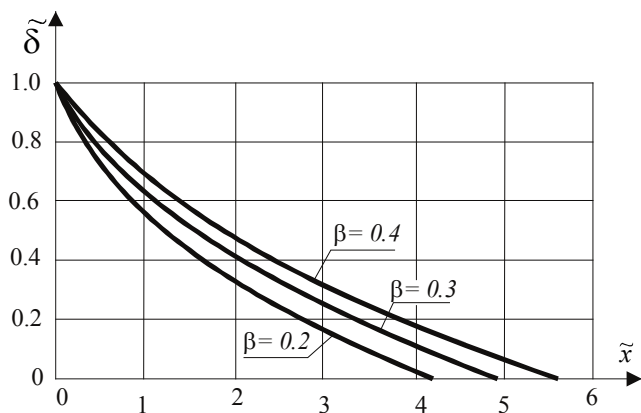


Fig. 5. Solidification front for $Pr = 0.01, Re=2000, Ste = 4, \tilde{a} = 1.0$ for not overheated liquid metals

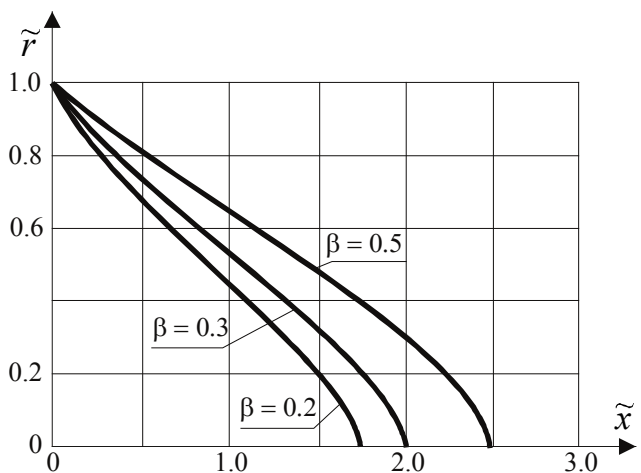


Fig. 6. Solidification front for $Pr = 0.01, Re=2000, Ste = 4, \tilde{a} = 1.0$ for not overheated liquid metals [9]

Figures 3-6 show shapes of the solidification front for different Reynolds numbers and given values of Pr, Ste, for different overheat parameters \mathcal{G} and different Biot numbers expressed by the parameters β . As it can easily be seen, the shape and size of the solidification front depend on the resistance of the contact layer $\lambda/(\alpha_{CON}H)$, the parameter \mathcal{G} , the Prandtl number Pr and the Reynolds number Rc. From the obtained solution it can be seen that the size of the solidification

front grows with increasing values of the Reynolds number, the Prandtl number, the resistance of the contact layer and the parameter \mathcal{G} .

As can be seen the maximum length of the liquid metal flow corresponds to the thickness $\tilde{\delta} = 0$ and is equal to

$$\tilde{x}_{max} = -\frac{Re \cdot Pr \cdot \tilde{a}}{Ste} \left[\frac{1}{\mathcal{G}} + \frac{1}{\mathcal{G}^2} \ln \frac{\mathcal{G}(\beta+1)-1}{\beta\mathcal{G}-1} \right]. \quad (17)$$

The elevation of the interface should not exceed the height of the mold. This may result in an interruption of the continuous casting process. In addition, the maximum length should satisfy the additional condition

$$\tilde{x}_{max} H \rho g < p_b, \quad (18)$$

which represents the supply of liquid metal to the mold and guarantees the continuity of the stream.

Figure 6 shows the shapes of the solidification fronts of the liquid metals for similar external conditions, that is, both at the same flow rates of the liquid metal and the same cooling conditions for comparison. It can be seen that the liquid silver solidifies faster than the liquid copper.

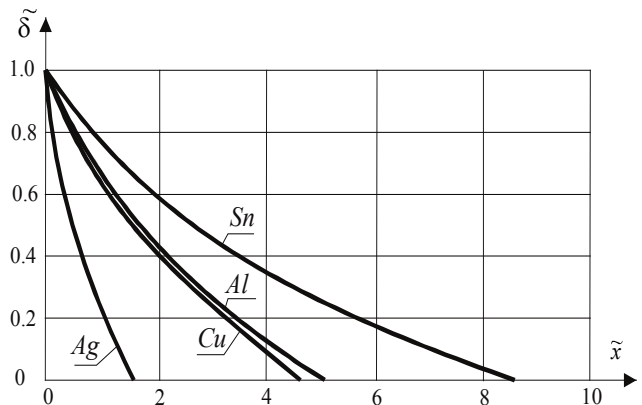


Fig. 7. Solidification front for not overheated liquid metals for $u = 0.1m/s, H = 0.01 m, \beta = 0.2, T_0=293K$

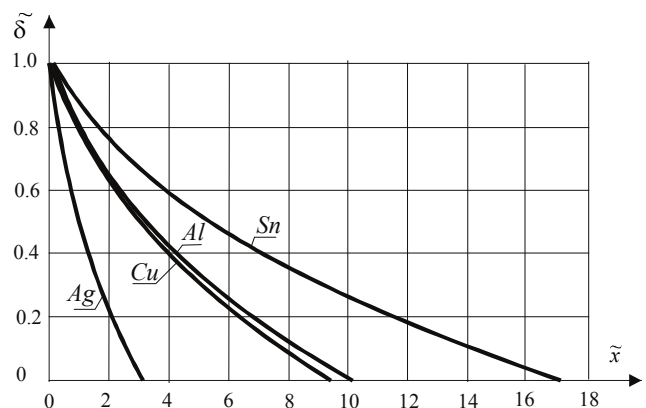


Fig. 8. Solidification front for not overheated liquid metals for $u = 0.2m/s, H = 0.01 m, \beta = 0.2, T_0=293K$

Tin is freezing slowly, so the solidification front is more elongated. Knowledge of the shape of the solidification front,

especially the maximum height of the solidification front x_{\max} , is very important and is needed for determining the technological parameters of the continuous process.

5. Conclusions

The paper is focused on the process of continuous casting of a thin metal plate in comparison with the continuous casting of thin metal rods. The solidification of pure liquid metal in an internal crystallizer flow is investigated and a simplified analytical model is presented. The role of the contact layer between the metal and the surface of the cooling channel is very important and might dominate the continuous casting of a thin metal plate. A simple analytical model is used to predict the freezing fronts for different metal flows. It is seen that these fronts might differ drastically, depending on the type of metal used. The shape of the solidified front depend on the shape of the casting form. Also the influence of the boundary conditions on the development of the frozen crust can nicely been studied with the simple model presented here.

REFERENCES

- [1] B. Mochnacki, B. Ortyl, Modelowanie numeryczne procesu odlewania ciągłego metodą wędrującego przekroju przy zmiennej w czasie siatce różnicowej, Zeszyty Naukowe Politechniki Śląskiej, Mechanika **62**, 37-43 (1978).
- [2] R. Grzymkowski, B. Mochnacki, Analiza krzepnięcia wlewka w procesie ciągłego odlewania stali, Krzepnięcie metali i stopów **2**, 69-125 (1980).
- [3] B. Mochnacki, J.S. Suchy, Modelowanie i symulacja krzepnięcia odlewów, PWN, Warszawa (1993).
- [4] B. Mochnacki, Application of the BEM for numerical modeling of continuous casting, Computational Mechanics 18, Springer-Verlag, 62-71 (1996).
- [5] A.K. Tieu, I.S. Kim, Simulation of the continuous casting process by mathematical model, Int. J. Mech. Sci. **39**, 2, 185-192 (1997).
- [6] E. Majchrzak, B. Mochnacki, M. Dziewoński, M. Jasiński, Identification of boundary heat flux on the continuous casting surface, Archives of Foundry Engineering **8**, 105-110 (2008).
- [7] L. Sowa, A. Bokota, Numerical model of thermal and flow phenomena the process growing of the CC slab, Archives of metallurgy and materials **56** 359-366 (2011).
- [8] J.S. Walker, E. Georgopoulos, Slow solidification of a cylinder with constant heat efflux, Int. Comm. Heat Mass Transfer **11**, 45-53 (1984).
- [9] Z. Lipnicki, K. Pantol, B. Weigand, Role of the contact layer on the continuous casting of thin metal rods, Archives of Metallurgy and Materials **58**, 2 (2013).
- [10] T. Loulou, E.A. Artyukhin, J.P. Bardon, Solidification of molten tin drop on a nickel substrate, 10th Int. Heat Transfer Conference, Brighton, UK **4**, 73-78 (1998).
- [11] T. Loulou, J.P. Artyukhin, J.P. Bardon, Estimation of thermal contact resistance during the first stages of metal solidification process: I – experiment principle and modelisation, Int. J. Heat and Mass Transfer **42**, 2119-2127 (1999).
- [12] T. Loulou, J.P. Artyukhin, J.P. Bardon, Estimation of thermal contact resistance during the first stages of metal solidification process: II – experimental setup and results, Int. J. Heat and Mass Transfer **42**, 2129-2142 (1999).
- [13] Z. Lipnicki, Role of the contact layer between liquid and solid on solidification process, Int. J. Heat and Mass Transfer **46**, 2149-2154 (2003).
- [14] Z. Lipnicki, B. Weigand, A. Bydalek, On the effect of a variable thermal contact resistance on the solidification process, Archives of Metallurgy and Materials **50**, 1055-1064 (2005).
- [15] Z. Lipnicki, B. Weigand, Influence of thermal boundary layer on the contact layer between a liquid and a cold plate in a solidification process, Heat and Mass Transfer **47**, 1629-1635 (2011).
- [16] Z. Lipnicki, B. Weigand, An experimental and theoretical study of solidification in a free-convection flow inside a vertical annular channel, Int. J. Heat and Mass Transfer **55**, 655–664 (2012).

Received: 20 January 2015.

